

Free electron laser in magnetars/Fast Radio Bursts

Maxim Lyutikov

Department of Physics and Astronomy, Purdue University, 525 Northwestern Avenue, West Lafayette, IN 47907-2036

ABSTRACT

We discuss coherent free electron laser (FEL) operating during explosive reconnection events in magnetized pair plasma of magnetar magnetospheres. The model explains many salient features of Fast Radio Bursts/magnetars' radio emission: temporal coincidence of radio and high energy bursts, high efficiency of conversion of plasma kinetic energy into coherent radiation, presence of variable, narrow-band emission features drifting down in frequency, high degree of linear polarization. The model relies on magnetar-specific drifting e^\pm plasma components (which generate wiggler field due to the development of the firehose instability) and the presence of reconnection-generated particle beam with mild Lorentz factor of $\gamma_b \sim$ few hundred.

1. Introduction

Generation of high brightness coherent emission by various types of neutron stars is a major unresolved problem in astrophysics – for nearly fifty years. One of the difficulty in identifying the process is that radio waves carry minuscule relative amount of the energy, $\sim 10^{-5}$ is typical. The phenomenon of Fast Radio Bursts challenges our understating of relativistic plasma coherent processes to the extreme. In this case radio waves can indeed carry astrophysically important amount of the energy (*e.g.*, radio luminosity can match, for a short period of time, the macroscopic Eddington luminosity). Still, the fraction emitted in radio remains small.

Detection of a radio burst from a Galactic magnetar by CHIME and STARE2 collaborations in coincidence with high energy bursts (The CHIME/FRB Collaboration et al. 2020; Bochenek et al. 2020; Mereghetti et al. 2020; Ridnaia et al. 2020; Tavani et al. 2020), and the similarity of it's properties to the Fast Radio Bursts (FRBs), gives credence to the magnetar origin of FRBs. The most compelling model, in our view, is the "Solar paradigm": generation of coherent radio emission during magnetospheric reconnection events (Lyutikov 2002; Popov & Postnov 2013; Lyutikov & Popov 2020)

In this paper we develop a novel, magnetar-specific, model for the generation of coherent emission during magnetospheric reconnection events. It relies on a process well studied in the context of laboratory plasma physics: free electron laser (FEL). Conceptually, many attempts to apply laboratory plasma process to astrophysical environments run into the “no engineer on site” problem: laboratory devices are often fine-tuned by engineers to produce the desired result; astrophysical lasers have to produce such fine-tuning naturally. As we argue below, magnetar magnetospheres may indeed naturally produce an analogue of the fine-tuned free electron laser.

2. Outline of the model: free electron laser in magnetar magnetospheres

The free electron lasers (Motz 1951; Madey 1971; Colson 1976; Deacon et al. 1977; Roberson & Sprangle 1989; Cohen et al. 1991) are operational laboratory devices that have high efficiency of energy transfer from the kinetic energy of particles to the coherent radiation. Let us first briefly outline the principles of FEL, in a regime relevant to magnetospheres of magnetars. FEL involves a fast relativistic electron beam propagating through periodically arranged magnets, the wiggler. In the moving reference frame of the beam, the wiggler magnetic field Lorentz-transforms into a backward propagating transverse electromagnetic wave. The wiggler’s magnetic field induces transverse oscillations of the electrons, and, most importantly longitudinal oscillations that lead to the creation of periodic density enhancements due to the ponderomotive force of the wiggler’s field. The collective backscatter of the wiggler-produced transverse wave by density perturbations leads to coherent emission of the antenna-type. (Antenna mechanism, in contrast to plasma maser, implies that each electron emits independently, but externally imposed perturbation – in this case the wiggler field - forces all the electrons emit in phase.) Most importantly this processes typically saturates at the level that a large fraction of the initial electron energy is converted into radiation.

Astrophysical applications of the FEL concept then require self-creation of the beam and the wiggler field. As we discuss below both conditions can be achieved during reconnection events in magnetar magnetospheres. First, the wiggler field is naturally produced as a firehose instability of counter-streaming plasma components on closed field lines of twisted magnetosphere of magnetars, §3. Second, reconnection events in the magnetosphere launch mildly fast particle beams, with Lorentz factor $\gamma_b \sim \text{few hundred}$. These beams propagating though the preexisting wiggler field produce FEL emission.

Magnetic fields in magnetars can reach quantum critical fields. At the same time we are interested in the production of coherent emission in the GHz range. Thus, the FEL in magnetospheres of magnetars will operate in the somewhat unusual regime of ultra-strong

guide field, when the cyclotron frequency $\omega_B = eB_0/(m_e c)$ (B_0 is the guide field) is much larger than the plasma frequency ω_p and the radiation frequency ω , $\omega_B \gg \omega_p, \omega$ (Manheimer & Ott 1974; Kwan & Dawson 1979; Friedland 1980; Ginzburg & Peskov 2013). In what follows we reconsider FEL operating in such dominant guide field.

3. Generation of a wiggler: pre-flare magnetosphere is unstable to firehose instability

3.1. Plasma flow in magnetar magnetospheres

Magnetars (Thompson & Duncan 1995; Thompson et al. 2002) (see Kaspi & Beloborodov 2017, for review) produce emission by dissipation of magnetic energy. Currents flowing in the non-potential magnetosphere produce emission in persistent state (corresponding to Anomalous X-ray pulsars, AXPs). Instabilities in the magnetosphere can lead to the generation of burst (observed as Soft Gamma-Ray repeaters, SGRs), similar to the case of Solar flares (Lyutikov 2015). Similarly to the Sun (Benz & Güdel 2010) radio emission can also be produced during X-ray flares (Lyutikov 2002; Lyutikov & Popov 2020).

Beloborodov (2013) developed a model of particle flow in (quasi) stationary states of magnetars. Briefly, the twist of the magnetic field lines frozen in the conducting crust generates a counter-streaming flow of e^\pm pair. The pair densities are related to the overall twist of the magnetosphere $\Delta\phi \leq 1$ and somewhat model-dependent plasma multiplicity $\mathcal{M} \sim 100$ (Thompson et al. 2002; Beloborodov 2013) The pre-flare plasma density can then be parametrized by the twist angle $\Delta\phi$ of the non-potential magnetic field and pair multiplicity \mathcal{M} (Thompson et al. 2002; Beloborodov 2013)

$$\begin{aligned} n_p &= \mathcal{M}(\Delta\phi) \frac{B}{4\pi er} = \kappa \frac{B}{4\pi er} \\ \kappa &= \mathcal{M}(\Delta\phi) \end{aligned} \tag{1}$$

where r is the local radial coordinate. The pair components stream with respect to each other with $\gamma_p \sim 100$ (Beloborodov 2013).

Next we demonstrate that such plasma is unstable to the generation of intense Alfvén waves via the firehose instability.

3.2. Firehose instability in magnetar magnetospheres

Let's assume that magnetospheric plasma is composed of two dense, oppositely charged beams with equal densities n_p and Lorentz factors γ_p . In the momentum rest frame, assuming charge neutrality, the dispersion relation for plasma (longitudinal) and transverse modes read (Melrose 1986, prob. 10.2)

$$1 - \frac{2\omega_p^2 (k^2 v^2 + \omega^2)}{\gamma_p^3 (\omega^2 - k^2 v^2)^2} = 0$$

$$\left(1 - \frac{k^2}{\omega^2} - \left(\frac{(\omega - kv)^2}{(\omega - kv)^2 - \frac{\omega_B^2}{\gamma_p^2}} + \frac{(\omega + kv)^2}{(\omega + kv)^2 - \frac{\omega_B^2}{\gamma_p^2}} \right) \frac{\omega_p^2}{\gamma_p \omega^2} \right)^2 - \left(\frac{\omega - kv}{(\omega - kv)^2 - \frac{\omega_B^2}{\gamma_p^2}} - \frac{\omega + kv}{(\omega + kv)^2 - \frac{\omega_B^2}{\gamma_p^2}} \right)^2 \frac{\omega_B^2 \omega_p^4}{\gamma_p^4 \omega^4} = 0 \quad (2)$$

(we set speed of light to unity).

The Langmuir plasma mode,

$$\omega_L^2 = k^2 v^2 + \left(1 \pm \sqrt{1 + \frac{4\gamma_p^3 k^2 v^2}{\omega_p^2}} \right) \frac{\omega_p^2}{\gamma_p^3} \quad (3)$$

(interestingly one the branches becomes subluminal for $k \geq \sqrt{2(1+v^2)\gamma_p\omega_p}$) shows two-stream instability for $k \leq \frac{\sqrt{3}\omega_p}{2\gamma_p^{3/2}v}$ with maximal growth rate

$$\Gamma_L = \frac{\omega_p}{2\gamma_p^{3/2}} \quad (4)$$

We are more interested in the transverse mode. In the limit $\omega_B \gg \omega_p, \omega$ and small k the dispersion becomes

$$\omega_t^2 = k^2 \left(1 \pm \frac{v\omega_p^2}{2k\omega_B} \right) \quad (5)$$

which shows the firehose instability for

$$k \leq \frac{2v\omega_p^2}{\omega_B} \quad (6)$$

The maximal growth rate is

$$k^* = \frac{v\omega_p^2}{\omega_B}$$

$$\Gamma_f = \frac{v\omega_p^2}{\omega_B} \quad (7)$$

We find for the growth rate and the wave number of the most unstable mode

$$\begin{aligned}\Gamma_f &\approx \kappa \frac{c}{r} \\ k^* &\approx \frac{\kappa}{r}\end{aligned}\tag{8}$$

The growth rate and the wavelength of the most unstable firehose mode are independent of the local magnetic field. This ensures that the model is applicable to a wide range of magnetars' magnetic fields.

Comparing the growth rate to the period of a neutron star Ω ,

$$\frac{\Gamma_f}{\Omega} = \kappa \frac{c}{\Omega r}\tag{9}$$

The minimal required twist-times-multiplicity parameter κ for magnetar-type periods near the surface is small

$$\kappa_{min} = \frac{\Omega r}{c} = 2 \times 10^{-4} P_s^{-1} \left(\frac{r}{R_{NS}} \right)\tag{10}$$

where P_s is a period of the neutron star in seconds. Hence we expect $\kappa \geq \kappa_{min}$ and the development of the instability.

In conclusion, we expect that persistent plasma flows in magnetar magnetospheres are unstable to firehose instability.

3.3. Saturation of the firehose instability

Non-resonant firehose instability excites long wavelength modes of magnetic field oscillations (low frequency Alfvén modes) with typical amplitude δB . Particles propagating through the wiggle field remain at lowest Landau level for $\omega_B \gg \gamma_p(k^*c)$: no cyclotron emission is generated. Particles propagating along the curved magnetic field lines will emit curvature emission in the typical radius of curvature $R_c \sim (k^*)^{-1}(B_0/\delta B)$. It may be demonstrated that the energy of the curvature emission produced during growth time of instability is tiny.

Thus, the initial energy of the relative motion is spent mostly on the generation of the fluctuating magnetic field δB :

$$\begin{aligned}2n_p \gamma_p m_e c^2 &\approx \frac{\delta B^2}{4\pi} \\ \delta B &= 4\sqrt{\pi} c \sqrt{n_p} \sqrt{m_e} \sqrt{\gamma_p} = 5 \times 10^5 b_q^{1/2} \gamma_p^{1/2} \kappa^{1/2} \left(\frac{r}{R_{NS}} \right)^{-2} \text{ Gauss}\end{aligned}\tag{11}$$

where $\lambda_C = \hbar/(m_e c)$ is the electron Compton wavelength and we normalized magnetic field to critical quantum field, $B_0 = b_q B_q$, $B_q = c^3 m_e^2 / (e \hbar)$. This is clearly an upper estimate on the intensity of the wiggler, as we neglected possible losses.

We expect that the mode with the highest growth rate at k^* will be dominant. This is an important assumption that needs to be verified via PIC simulations (Philippov priv. comm.)

4. Free electron laser during reconnection events in magnetar magnetospheres

4.1. Particle acceleration in reconnection events

Particle acceleration during reconnection events lately came to the forefront of high energy astrophysics. Particularly important was the observations of the Crab Nebula γ_p -ray flares by Fermi and AGILE Abdo et al. (2011); Tavani et al. (2011); Buehler et al. (2012), that in many ways are challenging our understanding of the importance of different particle acceleration mechanisms in astrophysical plasmas. These events offer tantalizing evidence in favor of relativistic reconnection Uzdensky et al. (2011); Clausen-Brown & Lyutikov (2012); Lyutikov et al. (2017b,a, 2018) operating in astrophysical sources.

Spectra of particles accelerated in reconnection events, obtained via PIC simulations, show a large variety, depending both on the plasma magnetization σ , and, importantly, overall configuration of the system (see below). First, in case of highly magnetized plasma with $\sigma \gg 1$ reconnection can produce very hard spectra $p \leq 2$ (where distribution function $f \propto \gamma_p^{-p}$, harder than the conventional limit $p \geq 2$ first-order Fermi acceleration at shocks (*e.g.* Blandford & Eichler 1987, non-linear effect can produce slightly smaller values). Reconnection in highly magnetized plasmas can naturally produce hard spectra with spectral index approaching $p \sim 1$ in the limit of large magnetizations Zenitani & Hoshino (2001); Guo et al. (2014); Sironi et al. (2015); Werner & Uzdensky (2017). Reconnection can then explain hard radio spectral indices $\alpha \sim 0.1 - 0.2$ in Pulsar Wind Nebulae (PWNe) Green (2014), as argued by Comisso & Sironi (2018); Lyutikov et al. (2019); Luo et al. (2020).

Second, large scale properties of the plasma configuration can also affect the particles' spectrum. On the one hand, most of work on particle acceleration in relativistic reconnection events use the initial set-up in the so-called ‘‘Harris equilibrium,’’ with magnetic field lines reversing over a microscopic (skin-depth-thick) current layer imposed as initial condition Zenitani & Hoshino (2001); Sironi & Spitkovsky (2014); Guo et al. (2014); Werner et al. (2016). In these result the newly formed magnetic X-points are ‘‘flat’’: as a result fast X-point acceleration regime is subdominant to island mergers (Comisso & Sironi 2018)

To overcome this problem Lyutikov et al. (2017a,b, 2018) investigated particle acceleration during *explosive relativistic reconnection*. In this case the reconnection is driven by large-scale stresses, rather than microscopic plasma effects. As a result, the collapsing X-Point have large opening angle: this leads to initial very efficient and fast acceleration of a few lucky particles to energies well beyond the initial mean energy per particle. This fast accelerated stage is then followed by a slower acceleration during island mergers.

Such a two-stage acceleration in reconnection can also generate the wiggler field: more dense slower components are unstable toward firehose instability, creating a wiggler field for the fast beams; then the fast beam produces coherent FEL emission. Highly non-stationary plasma process is needed in this scenario, since the wiggler needs to be generated before the high energy beams.

The magnetic energy per particle (the sigma parameter) in magnetar magnetospheres evaluates to

$$\sigma = \frac{B^2}{4\pi n m_e c^2} = \frac{R_{NS}}{\lambda_C} b_q \kappa^{-1} \left(\frac{r}{R_{NS}} \right)^{-2} = 10^{16} b_q \kappa^{-1} \left(\frac{r}{R_{NS}} \right)^{-2} \quad (12)$$

Modern PIC simulations do not come close to (12). This large σ also implies that the real Lorentz factors will be limited by other processes, not the average magnetic energy per particle or the available potential.

4.2. Kinematics of FEL

As discussed above, the pre-flare state is composed of two counter-streaming plasma beams, that became firehose unstable and generated an effective wiggler field. Reconnection event in the magnetosphere generates a fast beam propagating through this field. Next we consider beam dynamics in the wiggler dominated by the guide field. FEL with guide case has been previously considered by (Manheimer & Ott 1974; Kwan & Dawson 1979; Friedland 1980; Ginzburg & Peskov 2013). In magnetospheres of magnetars the FEL operates in the somewhat unusual regime of ultra-dominant strong guide field $\omega_B \gg \omega_p, \omega$. Below we re-derive the salient features of FEL in this unusual regime.

Consider a fast beam of density n_b propagating with Lorentz factor γ_b in the combined guide field B_0 and wiggler magnetic field δB . In the frame of the fast electron beam with $\gamma_b \gg 1$ the wiggler field looks nearly as a transverse electromagnetic wave with intensity $E'_w = \gamma_b \delta B$ and wavelength $k' \approx \gamma_b k^*$.

For a given beam Lorentz factor γ_b particles of the beam scatter the wiggler into high

frequency EM mode. The double-boosted frequency of the wiggler

$$\omega = 4\gamma_b^2(k^*c) = 4\gamma_b^2\kappa\frac{c}{r} \quad (13)$$

As the beam propagates up in the magnetosphere the emitted frequency decreases. This explains the frequency drifts observed in FRBs (Hessels et al. 2019; The CHIME/FRB Collaboration et al. 2019b,a; Josephy et al. 2019), as argued by Lyutikov (2020).

Given the wiggler’s wave vector k^* and the observed frequency ν_{ob} we can estimate beam’s Lorentz factor:

$$\gamma_b = \sqrt{\frac{\nu_{ob}}{2k^*c}} = \sqrt{\frac{\nu_{ob}r}{2\kappa c}} = 130\nu_9^{1/2}\kappa^{-1/2} \left(\frac{r}{R_{NS}}\right)^{1/2}, \quad (14)$$

a fairly mild Lorentz factor by pulsar standards (ν_9 is the observed frequency in GHz).

4.3. Magnetic undulator parameter

The conventional wave undulator parameter is

$$a = \frac{e\delta B}{k^*mc^2} \quad (15)$$

(in the absence of guide field this is a typical transverse momentum of the beam particles in units of $m_e c$). Using the estimate of the fluctuating magnetic field (11), the nonlinearity parameter a becomes

$$a = \left(\frac{4Ber\gamma_p}{c^2\kappa m_e}\right)^{1/2} = 2\sqrt{\frac{r}{\Lambda_C}} \left(\frac{\gamma_p b_q}{\kappa}\right)^{1/2} = 3 \times 10^8 \sqrt{\frac{b_q \gamma_p}{\kappa}} \left(\frac{r}{R_{NS}}\right)^{-1} \gg 1 \quad (16)$$

Similarly to δB , this is an upper limit.

In fact, the wiggler parameter for astrophysically-relevant case of guide-field dominated FEL is different. In the strongly guide-field dominated case we need to use magnetic undulator parameter a_B instead of a (Lyutikov 2017; Lyutikov & Rafat 2019).

Briefly, in the gyration frame of a particle subject to strong circularly polarized electromagnetic wave and the guide field, the amplitude of velocity oscillation v'_\perp follows from the equations of motion,

$$a = v'_\perp \left(\frac{1}{1 - v'^2_\perp} + \frac{\omega_{B_0}}{\omega'}\right) \quad (17)$$

(there are no z -oscillation in circularly polarized wave of constant amplitude.) In the absence of the guide field, $p_{\perp} = a$, while in the strongly guide-dominated case

$$\begin{aligned} v'_{\perp} \equiv a_B &= \frac{\delta B}{B} = 2\sqrt{\frac{\lambda_C}{r}} \left(\frac{\gamma_p \kappa}{b_q}\right)^{1/2} = 10^{-8} \left(\frac{\gamma_p \kappa}{b_q}\right)^{1/2} \left(\frac{r}{R_{NS}}\right)^{-1/2} \\ &= 10^{-8} \kappa^{1/2} \gamma_p^{1/2} b_q^{-1/2} \left(\frac{r}{R_{NS}}\right)^{-1/2} \ll 1 \end{aligned} \quad (18)$$

Parameter a_B is the typical transverse momentum (in units of $m_e c$) of a particle subject to strong electromagnetic wave in the dominant guide magnetic field. Qualitatively, in the presence of a guide field a particle accelerates in a field $\delta E \sim \delta B$ for time $\sim 1/\omega_B$, not $\sim 1/\omega$ as is the case of no guide field. In any astrophysically relevant case $a_B \ll 1$.

Since transverse magnetic field changes during the Lorentz boost, while the parallel remains the same, the magnetic undulator parameter a_B is not frame invariant. In the frame of the fast beam it is

$$a'_B = \gamma_b a_B \quad (19)$$

4.4. Beam dynamics in guide-field-dominated wiggler

Consider next beam dynamics in the field of linearly polarized wiggler field. For highly relativistic beam we can neglect the difference between beam velocity β_b and unity: the wiggler is then nearly an electromagnetic wave in the frame of the fast beam. We find then (primes denote values measured in the frame of the beam)

$$\begin{aligned} \mathbf{E}'_w &= E'_w \sin \xi \mathbf{e}_x \\ \mathbf{B}'_w &= E'_w \sin \xi \mathbf{e}_y + B_0 \mathbf{e}_z \\ \xi &= \omega'(t - z/\beta_b) \\ E'_w &= \gamma_b \delta B \end{aligned} \quad (20)$$

Since $p_{\perp}/(m_e c) \sim a_B \ll 1$ the transverse motion of particles induced by the wiggle is non-relativistic in the frame of the beam. We find for transverse components in the limit $v_z \ll 1$

$$\begin{aligned} v_y &= \frac{\omega_B \omega_{\delta} \sin \xi}{\omega'^2 - \omega_B^2} \approx -\frac{B'_w}{B} \sin \xi = -a_B \sin \xi \\ v_x &= \frac{\omega' \omega_{\delta} \cos \xi}{\omega_B^2 - \omega'^2} \approx \frac{B'_w}{B} \frac{\omega'}{\omega_B} \cos \xi = \frac{\omega'}{\omega_B} a_B \cos \xi \\ \omega_{\delta} &= \frac{e B'_w}{m_e c} \end{aligned} \quad (21)$$

Note that $v_y \gg v_x$: particles in the field of the wiggler move nearly linearly (this is an important fact for the resulting polarization.)

The longitudinal component, also non-relativistic,

$$v_z = \frac{\omega_\delta^2 \cos^2 \xi}{2(\omega_B^2 - \omega'^2)} = -\frac{\omega_\delta^2(1 + \cos(2\xi))}{4(\omega'^2 - \omega_B^2)} \approx \left(\frac{B'_w}{2B}\right)^2 (1 + \cos(2\xi)) = \frac{1 + \cos(2\xi)}{4} \gamma_b^2 a_B^2 \quad (22)$$

oscillates at the double frequency of the wiggler in the beam's frame.

4.5. Ponderomotive density enhancements

The wiggler field induces transverse oscillation of the beam. In addition, gradients of the wiggler's intensity in the beam's frame will induce longitudinal oscillations as we discuss next (see Freund & Drobot 1982, for more detailed discussion of particle trajectories in the combined fields of wiggler and guide field).

Given the axial velocity (22) charge conservation of the beam's particles,

$$\partial_t n_b + \partial_z (v_z n_b) = 0 \quad (23)$$

gives

$$\begin{aligned} n'_b(\xi) &= \frac{2\omega_\delta^2 n(\xi) \sin(2\xi)}{-4(\omega'^2 - \omega_B^2) + (1 + \cos(2\xi))\omega_\delta^2} \\ n'_b &= n'_{b,0} \left(\left(1 - \frac{\omega_\delta^2}{4(\omega'^2 - \omega_B^2)}\right) - \frac{\omega_\delta^2 \cos(2\xi)}{4(\omega'^2 - \omega_B^2)} \right) \approx \\ n'_{b,0} \left(1 + \frac{\omega_\delta^2 \cos(2\xi)}{4\omega_B^2}\right) &\approx n'_{b,0} \left(1 + \frac{B_w'^2}{4B_0^2} \cos(2\xi)\right) = n_{b,0} \left(1 + \gamma_b^2 \frac{a_B^2}{4} \cos(2\xi)\right) \end{aligned} \quad (24)$$

where $n'_{b,0}$ is the average beam density in its frame. One clearly recognizes this as density perturbations induced by the longitudinal ponderomotive force of the wiggler.

These charge oscillations of the beam particles should not be suppressed by Debye screening of the bulk plasma, hence we need the frequency of wiggler field in the beam's frame to be higher than the plasma frequency of the bulk plasma, measured in the beam's frame

$$\begin{aligned} \gamma_b(k^* c) &\geq \frac{\omega_p}{(\gamma_b \gamma_p)^{3/2}} \\ \gamma_b &\geq \left(\frac{Ber}{m_e c^2 \kappa \gamma_p^3}\right)^{1/5} = 2 \times 10^3 b_q^{1/5} \kappa^{-1/5} \gamma_p^{-3/5} \left(\frac{r}{R_{NS}}\right)^{-2/5}, \end{aligned} \quad (25)$$

a condition not too difficult to satisfy.

Thus, the wiggler introduces periodic density fluctuations in the fast beam, on the scale of the half wiggler wavelength (measured in the beam's rest frame).

4.6. Collective scattering of wiggler field by density inhomogeneities in the beam

As the beam propagates through the wiggler each beam particle scatters the wiggler field. Qualitatively, each scattering cross-section is enhanced by $1 + a^2$, but is suppressed by $(\omega/\omega_B)^2$ (Zeldovich 1975). Since the velocity oscillations are non-relativistic, Eq (21), the resulting cross-section σ_s for scattering is the conventional $\sigma_s \sim \sigma_T(\omega/\omega_B)^2$ (σ_T is Thompson cross-section, Blandford & Scharlemann 1976): high magnetic field suppresses electron-photon interaction.

The collective processes on the other hand can greatly amplify the wave-particles interactions. In particular, density perturbations of the beam (24) oscillate in phase in the field of the wiggler. As a result of coherent addition of emission of N particles confined to regions smaller than the wavelength and oscillating in phase, the final intensity scales as N^2 : this is the principle of the antenna mechanism of coherent emission.

As we discussed above, the ponderomotive force of the wiggler creates density enhancements in the beam on scales smaller than the emitted (scattered) wavelength, Eq. (24) and Fig. 1. These density enhancements oscillate coherently in the field of the wiggler, and emit (scatter) the wiggler's radiation in phase.

The wiggler wavelength in the frame of the beam is

$$\lambda_b^* = \frac{2\pi}{\gamma_b k^*} \quad (26)$$

If the beam density in the lab frame is a fraction of the plasma density (1), $n_b = \eta_b n_p$, beam density in the beam frame is

$$n'_b = \frac{n_b}{\gamma_b} = \eta_b \frac{n_p}{\gamma_b} \quad (27)$$

Density enhancement in the beam frame is

$$\delta n' = n'_b \frac{(\gamma_b \delta B)^2}{2B_0^2} = \frac{\eta_b \gamma_b a_B^2}{2} n_p \quad (28)$$

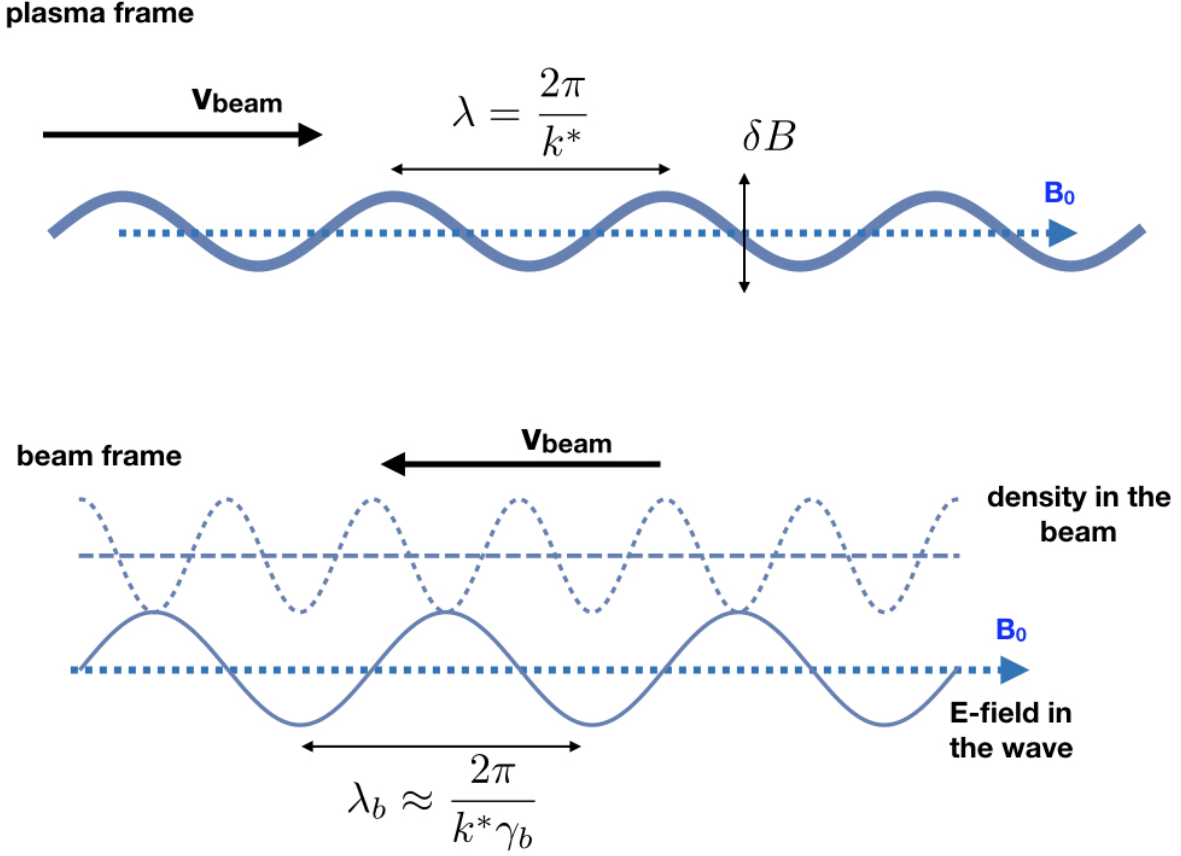


Fig. 1.— Propagation of fast beam through wiggler. In the wiggler frame the beam is propagating through perturbations with velocity v_{beam} . In the frame of the beam the wiggler is almost electromagnetic wave that induces ponderomotive density perturbations at double the frequency of the wiggler in the frame of the beam. High density regions of the beam oscillate in phase and coherently scatter the wiggler’s field.

Number of extra beam particles within the volume $\lambda_b^{*,3}$ is

$$N'_b = \lambda_b^{*,3} \delta n' = \gamma_p \eta_b \frac{m_e c^3}{\pi \nu_{ob}} = 10^{13} \gamma_p \eta_b \nu_9^{-1} \quad (29)$$

(this is an upper estimate on N'_b since density enhancement is limited just to a fraction of a wavelength). The number $N'_b \gg 1$ is the estimate of the coherent enhancement of the single-particle scattering of the wiggler field in the dominant guide magnetic field.

Emissivity per particle in the beam’s frame P' and in our frame P are then

$$P' \approx \frac{e^2 (\gamma_b \delta B)^2}{c B_0^2} N'_b$$

$$P \approx 2\gamma_b^2 P' = 32\pi\gamma_b^2 \gamma_p \eta_b \kappa \frac{m_e c^3}{r} \quad (30)$$

Using estimate (14) for the Lorentz factor of the beam we find a very simple relation for the coherent power of each beam particle

$$P \approx 16\pi\eta_b \gamma_p \nu m_e c^2 \quad (31)$$

The coherent power per particle (31) is extraordinary high. For example, for beam-plasma equipartition $\gamma_b n_b \approx \gamma_p n_p \rightarrow \eta_b = \gamma_p / \gamma_b$ relation (31) implies that a beam particle loses its energy to coherent emission in few oscillations. This is clearly an upper limit to the efficiency of coherent emission: recall that we used the upper limit on the wiggler’s strength, Eq (11), and upper limit on the number of coherently emitting particles, Eq (29). Also dispersive effects of the beam, and finite bandwidth of the saturated wiggler modes were neglected.

As mentioned above, calculations of the saturation levels of coherent instabilities is an exceptionally complicated procedure. Even with modern PIC methods very targeted types of simulations are needed to solidly assess the non-linear saturation level (since typically PICs use minimal resolution at plasma kinetic scales in an effort to capture larger scale dynamics.) Our estimates of the emitted power are encouraging.

5. FEL and FRB/magnetar phenomenology

The present model compares well with the observed FRB/magnetar phenomenology. The present model explains

- contemporaneous radio-high energy flares.
- high efficiency of conversion of particle energy into coherent radiation
- presence of narrow emission bands: it is related to the beam’s Lorentz factor and the wavelength of the wiggler field, Eq. (13)
- variable emission properties from the same source (*e.g.*, two sub-bursts in The CHIME/FRB Collaboration et al. 2020, had somewhat different spectra): mild variations of the beam Lorentz factor, or of the frequency of the wiggler, lead to different emitted frequencies, Eq. (13).

- intermittency of radio production: specific combination of parameters of bulk plasma, and of the beam is required for observed emission to be produced, and to fall into the typical observational range of radio telescopes
- downward frequency drifts observed in FRBs, (Hessels et al. 2019; The CHIME/FRB Collaboration et al. 2019b,a; Josephy et al. 2019). As the emission beam propagates in the magnetosphere the central frequency of the FEL decreases, Eq. (13), as argued previously by Lyutikov (2020).
- high linear polarization of FRBs (FRB 121102 and FRB 180916.J0158+65 show $\sim 100\%$ linear polarization, Michilli et al. 2018; CHIME/FRB Collaboration et al. 2019). In symmetric background pair plasma the wiggler is linearly polarized; in the particular FEL regime the motion of beam particles is also nearly one-dimensional, Eq. (21).

The FEL likely operates during initial stages of magnetar flares (there is tantalizing evidence that radio bursts lead X-ray bursts Mereghetti et al. 2020). It requires some minimal Lorentz factor of the beam, Eq. (14). This may explain why only some, very hard, X-ray flares (Ridnaia et al. 2020) are accompanied by radio bursts: the coherence condition is not satisfied in most of the bursts, only in those that produce a beam with sufficiently high Lorentz factor. Another limitation is that the wave number of the unstable firehose mode should be sufficiently high, see Eq. (8). This requires high twist angles $\Delta\phi$ and high multiplicities \mathcal{M} . In some sense, fine-tuning of parameters is required to occasionally produce radio emission. To address this question in more detail PIC simulations, including pair production, are needed.

6. Discussion

In this paper we discuss a novel, magnetar-specific, model of generation of coherent emission in magnetospheres of neutron stars: the free electron laser. We demonstrated first that the relative streaming of plasma component in magnetar magnetospheres is firehose unstable: this creates wiggler field that then scatters reconnection-produced fast beam.

The idea of a FEL in pulsar magnetosphere has been previously briefly discussed by Schopper et al. (2002); Fung & Kuijpers (2004). Schopper et al. (2002) discuss FEL on plasma Langmuir plasma turbulence generated by the two-stream Langmuir instability. Model of Langmuir turbulence on the open magnetic fields line of pulsar magnetospheres run into problem of insufficiently high growth rate (Cheng & Ruderman 1977; Usov 1986) (see review by Melrose 2017). On the open fields lines the plasma is moving with large bulk Lorentz

factor: this increases demands on the growth rate of the instability in the plasma frame. In addition, models based on the Langmuir waves excitation by the primary beam produced low growth rates due to the tenuous nature of the beam (with density only of the order of Goldreich-Julian), while models based on the relative streaming of the secondary plasma faced a problem that for high density of the secondary plasma the relative velocity develops slowly and remains small (Usov 1987).

Plasma flows in the magnetospheres of magnetars are different from the pulsars' open field lines: (i) plasma is not streaming with ultra-high Lorentz factor along the magnetic field (hence no suppression of instability due to bulk motion); (ii) larger densities are expected on twisted magnetic field lines, Eq. (1); (iii) large relative velocity of the streaming components is expected (Beloborodov 2013). As a result, transverse firehose perturbations are excited.

In terms of overall landscape of pulsar radio emission model, the present model falls under the “antenna” mechanism (as opposed to plasma maser Melrose 1986): all particles emit independently, but in phase. In laboratories this is achieved by the external driver through frequency or amplitude modulation, or prearranged configuration of the wiggler field, while in the case of magnetar magnetospheres the “driver” is the result of the plasma instability in the pre-flare configuration.

Acknowledgements

I would like to thank Andrei Beloborodov, Lorenzo Sironi and Alexander Philippov for discussions. This research was supported by NASA grant 80NSSC17K0757 and NSF grants 10001562 and 10001521.

REFERENCES

- Abdo, A. A., Ackermann, M., Ajello, M., Allafort, A., Baldini, L., Ballet, J., Barbiellini, G., & Bastieri, D. e. 2011, *Science*, 331, 739
- Beloborodov, A. M. 2013, *ApJ*, 777, 114
- Benz, A. O. & Güdel, M. 2010, *ARA&A*, 48, 241
- Blandford, R. & Eichler, D. 1987, *Phys. Rep.*, 154, 1
- Blandford, R. D. & Scharlemann, E. T. 1976, *MNRAS*, 174, 59

- Bochenek, C. D., Ravi, V., Belov, K. V., Hallinan, G., Kocz, J., Kulkarni, S. R., & McKenna, D. L. 2020, arXiv e-prints, arXiv:2005.10828
- Buehler, R., Scargle, J. D., Blandford, R. D., Baldini, L., Baring, M. G., Belfiore, A., Charles, E., Chiang, J., D’Ammando, F., Dermer, C. D., Funk, S., Grove, J. E., Harding, A. K., Hays, E., Kerr, M., Massaro, F., Mazziotta, M. N., Romani, R. W., Saz Parkinson, P. M., Tennant, A. F., & Weisskopf, M. C. 2012, *ApJ*, 749, 26
- Cheng, A. F. & Ruderman, M. A. 1977, *ApJ*, 212, 800
- CHIME/FRB Collaboration, Andersen, B. C., Bandura, K., Bhardwaj, M., Boubel, P., Boyce, M. M., Boyle, P. J., Brar, C., Cassanelli, T., Chawla, P., Cubranic, D., Deng, M., Dobbs, M., Fandino, M., Fonseca, E., Gaensler, B. M., Gilbert, A. J., Giri, U., Good, D. C., Halpern, M., Hill, A. S., Hinshaw, G., Höfer, C., Josephy, A., Kaspi, V. M., Kothes, R., Landecker, T. L., Lang, D. A., Li, D. Z., Lin, H. H., Masui, K. W., Mena-Parra, J., Merryfield, M., Mckinven, R., Michilli, D., Milutinovic, N., Naidu, A., Newburgh, L. B., Ng, C., Patel, C., Pen, U., Pinsonneault-Marotte, T., Pleunis, Z., Rafiei-Ravandi, M., Rahman, M., Ransom, S. M., Renard, A., Scholz, P., Siegel, S. R., Singh, S., Smith, K. M., Stairs, I. H., Tendulkar, S. P., Tretyakov, I., Vanderlinde, K., Yadav, P., & Zwaniga, A. V. 2019, *ApJ*, 885, L24
- Clausen-Brown, E. & Lyutikov, M. 2012, *MNRAS*, 426, 1374
- Cohen, B. I., Cohen, R. H., Nevins, W. M., & Rognlien, T. D. 1991, *Reviews of Modern Physics*, 63, 949
- Colson, W. B. 1976, *Physics Letters A*, 59, 187
- Comisso, L. & Sironi, L. 2018, *Phys. Rev. Lett.*, 121, 255101
- Deacon, D. A. G., Elias, L. R., Madey, J. M. J., Ramian, G. J., Schwettman, H. A., & Smith, T. I. 1977, *Phys. Rev. Lett.*, 38, 892
- Freund, H. P. & Drobot, A. T. 1982, *Physics of Fluids*, 25, 736
- Friedland, L. 1980, *Physics of Fluids*, 23, 2376
- Fung, P. K. & Kuijpers, J. 2004, *A&A*, 422, 817
- Ginzburg, N. S. & Peskov, N. Y. 2013, *Physical Review Accelerators and Beams*, 16, 090701
- Green, D. A. 2014, *Bulletin of the Astronomical Society of India*, 42, 47
- Guo, F., Li, H., Daughton, W., & Liu, Y.-H. 2014, *Physical Review Letters*, 113, 155005

- Hessels, J. W. T., Spitler, L. G., Seymour, A. D., Cordes, J. M., Michilli, D., Lynch, R. S., Gourdji, K., Archibald, A. M., Bassa, C. G., Bower, G. C., Chatterjee, S., Connor, L., Crawford, F., Deneva, J. S., Gajjar, V., Kaspi, V. M., Keimpema, A., Law, C. J., Marcote, B., McLaughlin, M. A., Paragi, Z., Petroff, E., Ransom, S. M., Scholz, P., Stappers, B. W., & Tendulkar, S. P. 2019, *ApJ*, 876, L23
- Josephy, A., Chawla, P., Fonseca, E., Ng, C., Patel, C., Pleunis, Z., Scholz, P., Andersen, B. C., Bandura, K., Bhardwaj, M., Boyce, M. M., Boyle, P. J., Brar, C., Cubranic, D., Dobbs, M., Gaensler, B. M., Gill, A., Giri, U., Good, D. C., Halpern, M., Hinshaw, G., Kaspi, V. M., Landecker, T. L., Lang, D. A., Lin, H. H., Masui, K. W., Mckinven, R., Mena-Parra, J., Merryfield, M., Michilli, D., Milutinovic, N., Naidu, A., Pen, U., Rafei-Ravand i, M., Rahman, M., Ransom, S. M., Renard, A., Siegel, S. R., Smith, K. M., Stairs, I. H., Tendulkar, S. P., Vanderlinde, K., Yadav, P., & Zwaniga, A. V. 2019, arXiv e-prints, arXiv:1906.11305
- Kaspi, V. M. & Beloborodov, A. M. 2017, *ARA&A*, 55, 261
- Kwan, T. & Dawson, J. M. 1979, *Physics of Fluids*, 22, 1089
- Luo, Y., Lyutikov, M., Temim, T., & Comisso, L. 2020, arXiv e-prints, arXiv:2005.06319
- Lyutikov, M. 2002, *ApJ*, 580, L65
- . 2015, *MNRAS*, 447, 1407
- . 2017, *ApJ*, 838, L13
- . 2020, *ApJ*, 889, 135
- Lyutikov, M., Komissarov, S., & Sironi, L. 2018, *Journal of Plasma Physics*, 84, 635840201
- Lyutikov, M. & Popov, S. 2020, arXiv e-prints, arXiv:2005.05093
- Lyutikov, M. & Rafat, M. 2019, arXiv e-prints, arXiv:1901.03260
- Lyutikov, M., Sironi, L., Komissarov, S. S., & Porth, O. 2017a, *Journal of Plasma Physics*, 83, 635830601
- . 2017b, *Journal of Plasma Physics*, 83, 635830602
- Lyutikov, M., Temim, T., Komissarov, S., Slane, P., Sironi, L., & Comisso, L. 2019, *MNRAS*, 489, 2403
- Madey, J. M. J. 1971, *Journal of Applied Physics*, 42, 1906

- Manheimer, W. M. & Ott, E. 1974, *Physics of Fluids*, 17, 463
- Melrose, D. B. 1986, *Instabilities in Space and Laboratory Plasmas*
- . 2017, *Reviews of Modern Plasma Physics*, 1, 5
- Mereghetti, S., Savchenko, V., Ferrigno, C., Götz, D., Rigoselli, M., Tiengo, A., Bazzano, A., Bozzo, E., Coleiro, A., Courvoisier, T. J. L., Doyle, M., Goldwurm, A., Hanlon, L., Jourdain, E., von Kienlin, A., Lutovinov, A., Martin-Carrillo, A., Molkov, S., Natalucci, L., Onori, F., Panessa, F., Rodi, J., Rodriguez, J., Sánchez-Fernández, C., Sunyaev, R., & Ubertini, P. 2020, arXiv e-prints, arXiv:2005.06335
- Michilli, D., Seymour, A., Hessels, J. W. T., Spitler, L. G., Gajjar, V., Archibald, A. M., Bower, G. C., Chatterjee, S., Cordes, J. M., Gourdji, K., Heald, G. H., Kaspi, V. M., Law, C. J., Sobey, C., Adams, E. A. K., Bassa, C. G., Bogdanov, S., Brinkman, C., Demorest, P., Fernandez, F., Hellbourg, G., Lazio, T. J. W., Lynch, R. S., Maddox, N., Marcote, B., McLaughlin, M. A., Paragi, Z., Ransom, S. M., Scholz, P., Siemion, A. P. V., Tendulkar, S. P., van Rooy, P., Wharton, R. S., & Whitlow, D. 2018, *Nature*, 553, 182
- Motz, H. 1951, *Journal of Applied Physics*, 22, 527
- Popov, S. B. & Postnov, K. A. 2013, arXiv e-prints, arXiv:1307.4924
- Ridnaia, A., Svinkin, D., Frederiks, D., Bykov, A., Popov, S., Aptekar, R., Golenetskii, S., Lysenko, A., Tsvetkova, A., Ulanov, M., & Cline, T. 2020, arXiv e-prints, arXiv:2005.11178
- Roberson, C. W. & Sprangle, P. 1989, *Physics of Fluids B*, 1, 3
- Schopper, R., Ruhl, H., Kunzl, T. A., & Lesch, H. 2002, in *Neutron Stars, Pulsars, and Supernova Remnants*, ed. W. Becker, H. Lesch, & J. Trümper, 193–+
- Sironi, L., Petropoulou, M., & Giannios, D. 2015, *MNRAS*, 450, 183
- Sironi, L. & Spitkovsky, A. 2014, *ApJ*, 783, L21
- Tavani, M., Bulgarelli, A., Vittorini, V., Pellizzoni, A., Striani, E., Caraveo, P., Weisskopf, M. C., & Tennant, A. e. 2011, *Science*, 331, 736
- Tavani, M., Casentini, C., Ursi, A., Verrecchia, F., Addis, A., Antonelli, L. A., Argan, A., Barbiellini, G., Baroncelli, L., Bernardi, G., Bianchi, G., Bulgarelli, A., Caraveo, P., Cardillo, M., Cattaneo, P. W., Chen, A. W., Costa, E., Del Monte, E., Di Cocco,

G., Di Persio, G., Donnarumma, I., Evangelista, Y., Feroci, M., Ferrari, A., Fioretti, V., Fuschino, F., Galli, M., Gianotti, F., Giuliani, A., Labanti, C., Lazzarotto, F., Lipari, P., Longo, F., Lucarelli, F., Magro, A., Marisaldi, M., Mereghetti, S., Morelli, E., Morselli, A., Naldi, G., Pacciani, L., Parmiggiani, N., Paoletti, F., Pellizzoni, A., Perri, M., Perotti, F., Piano, G., Picozza, P., Pilia, M., Pittori, C., Puccetti, S., Pupillo, G., Rapisarda, M., Rappoldi, A., Rubini, A., Setti, G., Soffitta, P., Trifoglio, M., Trois, A., Vercellone, S., Vittorini, V., Giommi, P., & D' Amico, F. 2020, arXiv e-prints, arXiv:2005.12164

The CHIME/FRB Collaboration, :, Andersen, B. C., Bandura, K., Bhardwaj, M., Boubel, P., Boyce, M. M., Boyle, P. J., Brar, C., Cassanelli, T., Chawla, P., Cubranic, D., Deng, M., Dobbs, M., Fandino, M., Fonseca, E., Gaensler, B. M., Gilbert, A. J., Giri, U., Good, D. C., Halpern, M., Höfer, C., Hill, A. S., Hinshaw, G., Josephy, A., Kaspi, V. M., Kothes, R., Landecker, T. L., Lang, D. A., Li, D. Z., Lin, H. H., Masui, K. W., Mena-Parra, J., Merryfield, M., Mckinven, R., Michilli, D., Milutinovic, N., Naidu, A., Newburgh, L. B., Ng, C., Patel, C., Pen, U., Pinsonneault-Marotte, T., Pleunis, Z., Rafiei-Ravandi, M., Rahman, M., Ransom, S. M., Renard, A., Scholz, P., Siegel, S. R., Singh, S., Smith, K. M., Stairs, I. H., Tendulkar, S. P., Tretyakov, I., Vanderlinde, K., Yadav, P., & Zwaniga, A. V. 2019a, arXiv e-prints, arXiv:1908.03507

The CHIME/FRB Collaboration, :, Andersen, B. C., Bandura, K. M., Bhardwaj, M., Bij, A., Boyce, M. M., Boyle, P. J., Brar, C., Cassanelli, T., Chawla, P., Chen, T., Cliche, J. F., Cook, A., Cubranic, D., Curtin, A. P., Denman, N. T., Dobbs, M., Dong, F. Q., Fandino, M., Fonseca, E., Gaensler, B. M., Giri, U., Good, D. C., Halpern, M., Hill, A. S., Hinshaw, G. F., Höfer, C., Josephy, A., Kania, J. W., Kaspi, V. M., Landecker, T. L., Leung, C., Li, D. Z., Lin, H. H., Masui, K. W., Mckinven, R., Mena-Parra, J., Merryfield, M., Meyers, B. W., Michilli, D., Milutinovic, N., Mirhosseini, A., Münchmeyer, M., Naidu, A., Newburgh, L. B., Ng, C., Patel, C., Pen, U. L., Pinsonneault-Marotte, T., Pleunis, Z., Quine, B. M., Rafiei-Ravandi, M., Rahman, M., Ransom, S. M., Renard, A., Sanghavi, P., Scholz, P., Shaw, J. R., Shin, K., Siegel, S. R., Singh, S., Smegal, R. J., Smith, K. M., Stairs, I. H., Tan, C. M., Tendulkar, S. P., Tretyakov, I., Vanderlinde, K., Wang, H., Wulf, D., & Zwaniga, A. V. 2020, arXiv e-prints, arXiv:2005.10324

The CHIME/FRB Collaboration, Amiri, M., Bandura, K., Bhardwaj, M., Boubel, P., Boyce, M. M., Boyle, P. J., . Brar, C., Burhanpurkar, M., Cassanelli, T., Chawla, P., Cliche, J. F., Cubranic, D., Deng, M., Denman, N., Dobbs, M., Fandino, M., Fonseca, E., Gaensler, B. M., Gilbert, A. J., Gill, A., Giri, U., Good, D. C., Halpern, M., Hanna, D. S., Hill, A. S., Hinshaw, G., Höfer, C., Josephy, A., Kaspi, V. M., Landecker, T. L.,

- Lang, D. A., Lin, H. H., Masui, K. W., Mckinven, R., Mena-Parra, J., Merryfield, M., Michilli, D., Milutinovic, N., Moatti, C., Naidu, A., Newburgh, L. B., Ng, C., Patel, C., Pen, U., Pinsonneault-Marotte, T., Pleunis, Z., Rafiei-Ravandi, M., Rahman, M., Ransom, S. M., Renard, A., Scholz, P., Shaw, J. R., Siegel, S. R., Smith, K. M., Stairs, I. H., Tendulkar, S. P., Tretyakov, I., Vanderlinde, K., & Yadav, P. 2019b, *Nature*, 566, 235
- Thompson, C. & Duncan, R. C. 1995, *MNRAS*, 275, 255
- Thompson, C., Lyutikov, M., & Kulkarni, S. R. 2002, *ApJ*, 574, 332
- Usov, V. V. 1986, *Astronomicheskij Tsirkulyar*, 1431, 1
- . 1987, *ApJ*, 320, 333
- Uzdensky, D. A., Cerutti, B., & Begelman, M. C. 2011, *ApJ*, 737, L40
- Werner, G. R. & Uzdensky, D. A. 2017, *ApJ*, 843, L27
- Werner, G. R., Uzdensky, D. A., Cerutti, B., Nalewajko, K., & Begelman, M. C. 2016, *ApJ*, 816, L8
- Zeldovich, I. B. 1975, *Uspekhi Fizicheskikh Nauk*, 115, 161
- Zenitani, S. & Hoshino, M. 2001, *ApJ*, 562, L63